

Water Resources Research

RESEARCH ARTICLE

10.1029/2024WR038308

Global River Topology (GRIT): A Bifurcating River Hydrography



Key Points:

- Existing large-scale river networks only represent single-threaded gravity flow paths, rather than observed river centerlines
- Global River Topology (GRIT) was created by merging the 30 m Landsat-based river mask from Global River Widths from Landsat with elevation streams, using the new 30 m FABDEM for greater accuracy
- GRIT is the first branching global river network representing bifurcations, multi-threaded channels, and canals

Supporting Information:

Supporting Information may be found in the online version of this article.

Correspondence to:

M. Wortmann,
michel.wortmann@ecmwf.int

Citation:

Wortmann, M., Slater, L., Hawker, L., Liu, Y., Neal, J., Zhang, B., et al. (2025). Global River Topology (GRIT): A bifurcating river hydrography. *Water Resources Research*, 61, e2024WR038308. <https://doi.org/10.1029/2024WR038308>

Received 28 JUN 2024

Accepted 7 MAR 2025

Author Contributions:

Conceptualization: M. Wortmann

Data curation: M. Wortmann

Formal analysis: M. Wortmann, L. Hawker

















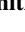


Funding acquisition: L. Slater, J. Neal, P. Ashworth, H. Cloke, J. Leyland, S. McLelland, A. P. Nicholas, G. Sambrook-Smith, D. Parsons, S. E. Darby

Investigation: M. Wortmann

Methodology: M. Wortmann

Software: M. Wortmann, J. Schwenk

Supervision: L. Slater

M. Wortmann^{1,2} , L. Slater¹ , L. Hawker³ , Y. Liu¹ , J. Neal³ , B. Zhang¹ , J. Schwenk⁴ , G. Allen⁵ , P. Ashworth⁶ , R. Boothroyd⁷ , H. Cloke^{8,9} , P. Delorme¹⁰ , S. H. Gebrechorkos^{1,11} , H. Griffith¹² , J. Leyland¹¹ , S. McLelland¹³ , A. P. Nicholas¹⁴, G. Sambrook-Smith¹⁵ , E. Vahidi¹⁴, D. Parsons¹⁶ , and S. E. Darby¹¹ 

¹School of Geography and the Environment, University of Oxford, Oxford, UK, ²European Centre for Medium-Range Weather Forecasts, Reading, UK, ³School of Geographical Sciences, University of Bristol, Bristol, UK, ⁴Information Systems and Modeling Division, Los Alamos National Laboratory, Los Alamos, NM, USA, ⁵Department of Geosciences, Virginia Polytechnic Institute and State University, Blacksburg, VA, USA, ⁶School of Applied Sciences, University of Brighton, Sussex, UK, ⁷Department of Geography and Planning, University of Liverpool, Liverpool, UK, ⁸Department of Meteorology, University of Reading, Reading, UK, ⁹Department of Geography and Environmental Science, University of Reading, Reading, UK, ¹⁰Laboratoire de Géologie, École Normale Supérieure, PSL, Paris, France, ¹¹School of Geography and Environmental Science, University of Southampton, Southampton, UK, ¹²JBA Consulting, Skipton, UK, ¹³Energy and Environment Institute, University of Hull, Hull, UK, ¹⁴Geography, Faculty of Environment, Science and Economy, University of Exeter, Exeter, UK, ¹⁵School of Geography, Earth, Environmental Sciences, University of Birmingham, Birmingham, UK, ¹⁶Vice Chancellor's Office, Loughborough University, Loughborough, UK

Abstract Existing global river networks underpin a wide range of hydrological applications but do not represent channels with divergent river flows (bifurcations, multi-threaded channels, canals), as these features defy the convergent flow assumption that elevation-derived networks (e.g., HydroSHEDS, MERIT Hydro) are based on. Yet, bifurcations are important features of the global river drainage system, especially on large floodplains and river deltas, and are also often found in densely populated regions. Here we developed the first raster and vector-based Global River Topology that not only represents the tributaries of the global drainage network but also the distributaries, including multi-threaded rivers, canals and deltas. We achieve this by merging a 30 m Landsat-based river mask with elevation-generated streams to ensure a homogeneous drainage density outside of the river mask for rivers narrower than approximately 30 m. Crucially, we employ the new 30 m digital terrain model, FABDEM, based on TanDEM-X, which shows greater accuracy over the traditionally used SRTM derivatives. After vectorization and pruning, directionality is assigned by a series of elevation, flow angle and continuity approaches. The new global network and its attributes are validated using gauging stations, comparison with existing networks, and randomized manual checks. The new network represents 19.6 million km of streams and rivers with drainage areas greater than 50 km² and includes 67,495 bifurcations. With the advent of hyper-resolution modeling and artificial intelligence, GRIT is expected to greatly improve the accuracy of many river-based applications such as flood forecasting, water availability and quality simulations, or riverine habitat mapping.

Plain Language Summary Global river maps often overlook complex features, such as when a single river channel splits into multiple channels. These branching river systems are important because they are often found in densely populated, often flood-prone regions, and they are crucial for understanding water movement across the Earth's surface. To address this limitation of existing river maps, we developed a new global river network called Global River Topology (GRIT), which includes these branching rivers and channels. GRIT was created by combining high-resolution satellite imagery of rivers with advanced elevation data of the earth's surface. GRIT not only includes the main river channels but also provides information on river flow directions, widths, and points where rivers split. The GRIT river network has a total length of 19.6 million km and includes 67,495 bifurcations. GRIT stands to significantly enhance applications in hydrology, ecology, geomorphology, and flood management.

1. Introduction

River networks underpin many large-scale analyses in the environmental sciences and geosciences, such as global and regional flood inundation modeling (Alfieri et al., 2014; Hirabayashi et al., 2013; Yamazaki et al., 2011), as

© 2025. The Author(s). *Water Resources Research* published by Wiley Periodicals LLC on behalf of American Geophysical Union.

This is an open access article under the terms of the [Creative Commons Attribution License](https://creativecommons.org/licenses/by/4.0/), which permits use, distribution and reproduction in any medium, provided the original work is properly cited.

Validation: M. Wortmann, L. Slater, L. Hawker, Y. Liu, B. Zhang
Visualization: M. Wortmann, L. Hawker, Y. Liu
Writing – original draft: M. Wortmann, L. Slater, L. Hawker, J. Neal
Writing – review & editing: L. Slater, L. Hawker, Y. Liu, J. Neal, B. Zhang, J. Schwenk, G. Allen, P. Ashworth, R. Boothroyd, H. Cloke, P. Delorme, S. H. Gebrechorkos, H. Griffith, J. Leyland, S. McLelland, A. P. Nicholas, G. Sambrook-Smith, E. Vahidi, D. Parsons, S. E. Darby

well as hydrological (Gebrechorkos et al., 2024; Gosling et al., 2017; Lin et al., 2019; Yang et al., 2021), biogeochemical (Liu et al., 2022; Raymond et al., 2013), ecological (Fatichi et al., 2016) and sediment (Cohen et al., 2013) modeling. The accuracy of the data sets underpinning these analyses is essential to support large-scale investigations of global environmental problems. For example, at a global scale, fluvial floods remain fatal and costly (Doocy et al., 2013) and damaging floods are likely to increase in many regions of the world with climate change (Dottori et al., 2018).

1.1. Limitations of Existing Global Hydrographies

Existing global river hydrographies presuppose downstream runoff convergence, relying on surface elevation data to depict only tributary drainage systems (Lehner et al., 2008; USGS, 2001; Yamazaki et al., 2019). However, this assumption of downstream runoff convergence fails in many river basins, particularly in regions attracting human habitation, such as lowland floodplains and deltas. Many river basins in fact contain multi-threaded, anabranching and distributary river systems of both natural and anthropogenic origin, although the total extent of divided channels remains unquantified at the global scale. HYDRO1k provided the first global hydrographic data set at 1 km resolution (USGS, 2001). Later, Lehner et al. (2008) created an extensively quality-checked hydrographic data set from 3 arc-second (~90 m) Shuttle Radar Topography Mission (SRTM) elevation data. More recently, the SRTM-based Multi-Error-Removed Improved-Terrain hydrography (MERIT-Hydro) has become widely used, as it assimilates a collection of global ancillary data sets to improve the accuracy of drainage paths and terrain elevations (Yamazaki et al., 2017, 2019). The latter was also used to derive river networks with smaller and variable drainage densities and/or extended attributes (Amatulli et al., 2022; Lin et al., 2021; Yan et al., 2019). To date, the only global river network that does not rely on elevation data is the vector product of the Global River Widths from Landsat (GRWL) data, which includes rivers wider than 30 m as well as large bifurcations and canals (Allen & Pavelsky, 2018a, 2018b). The GRWL product was recently enhanced to form the SWORD network for use with the Surface Water and Ocean Topography (SWOT) satellite mission, which included gap filling and the association of drainage area from MERIT-Hydro (Altenau et al., 2021a, 2021b). However, SWORD is not a multi-threaded network, does not include rivers smaller than 30 m width, misses many river branches and still relies on the tributary-only hydrography of MERIT-Hydro.

A further weakness of the aforementioned hydrographies is that they are based on outdated (Bielski et al., 2024) Digital Elevation Models (DEMs), that is, mainly the Shuttle Radar Topography Mission (SRTM) DEM acquired in 2000 with a reported mean absolute vertical accuracy of ~6 m (Rodriguez et al., 2006). A newer, more accurate, DEM called Copernicus DEM has since been made publicly available by the European Space Agency (ESA), presenting an opportunity to create an improved hydrographic data set. The TanDEM-X based Copernicus-DEM is globally available at 1 arc-second (~30 m) resolution and has recently been corrected to remove forests and buildings and released as FABDEM (Hawker et al., 2022) with mean absolute vertical errors in built-up areas of 1.12 m, and in forests of 2.88 m. FABDEM's 30 m spatial resolution is finer than that of the Shuttle Radar Topography Mission (SRTM) derived DEMs (3 arc s ~90 m) used in other global hydrographies (e.g., HydroSHEDS and MERIT-Hydro). Moreover, numerous recent studies have also found FABDEM to be the most accurate global terrain data set at the time of writing (Bielski et al., 2024; Marsh et al., 2023; Meadows et al., 2024).

1.2. Existing Branching River Networks at Local to National Scales

Branching river networks exist on local to national scales, such as fully directed distributary networks (Dong et al., 2020; Schwenk et al., 2020) or national scale networks that include multiple river branches and artificial channels (Moore et al., 2019; Ordnance Survey, 2022). At the national scale, the National Hydrography Dataset Plus (NHDPlus) data of the United States is a prominent example of a highly detailed, directed and attribute-enriched national river network that includes a list of ancillary hydrographic data sets (David et al., 2011; Moore et al., 2019). NHDPlus was built from national infrastructure vector data sets, is subject to continuous, manual quality assurance and includes many complex flow paths, artificial conduits and canals. At the reach or delta scale, studies on multi-threaded river systems (Coffey & Shaw, 2017; Jerolmack & Swenson, 2007; Schwenk et al., 2020) have also progressed independently from elevation-based hydrographic data sets. Examples include topological investigations, mainly concerned with directionality (Chen et al., 2022; Schwenk et al., 2020), and morphological studies, mainly concerned with delta evolution and flow partitioning (Dong et al., 2020;

Jerolmack & Swenson, 2007) or the delta data set DIDNT (Hariharan et al., 2022). However, none of these local and national networks have been integrated into continental scale hydrographic data sets.

1.3. GRIT: The First Global High-Resolution, Branching River Network

Combining methods and results from both local- to regional-scale distributary network research and global DEM-generated hydrographic data sets, this work seeks to produce the first global hydrography that includes tributary and distributary rivers, contrary to existing global data sets (Amatulli et al., 2022; Bierkens et al., 2015; Carlson et al., 2024; Lehner & Grill, 2013; Wood et al., 2011; Yamazaki et al., 2017). The 30 m river mask of GRWL and the ~30 m FABDEM serve as the primary input data sets to produce the first globally consistent hydrography at ~30 m raster resolution and a vector river network, based on a combination of river mask vectorization and traditional stream-burning approaches. A global collection of river gauging stations, reference river networks and randomized manual inspections of high-resolution satellite imagery are used to validate the data set.

The resulting GRIT river network is a topographically accurate, bifurcating river network which supports a variety of novel use cases. GRIT is well-suited for data-driven or machine learning applications such as large-sample streamflow modeling and forecasting. Catchment-scale climatic and geophysical attributes from observational, reanalysis, and environmental data sets can be extracted for every ~1 km reach of the GRIT network. Machine learning models trained on observational streamflow records, such as the GRDC, can then be used to issue streamflow predictions at the global scale, including in ungauged regions (e.g., Liu et al., 2024). A second application of the GRIT network is more accurate global hydrodynamic modeling in regions with bifurcating river systems and deltas. Lastly, a third application of GRIT is enhanced mapping of ecological habitats in bifurcating river systems.

Here, we describe the methods used to develop the GRIT river network and introduce the data products (Section 2), evaluate GRIT (Section 3), and discuss the implications and limitations of the work (Section 4), before concluding (Section 5).

2. Materials and Methods

We combine state-of-the-art methods from distributary network analysis and global tributary hydrographies to produce the GRIT network (Figure 1). Detailed descriptions of the input data sets and methods used are found below.

2.1. River Mask Creation

We employ the Global River Width from Landsat (GRWL) data set (Allen & Pavelsky, 2018a) as our water extent data set. Despite recent advances in the ability of global DEMs to represent global terrain, there are still inaccuracies in elevation that can have significant impacts on hydrologic applications (Bielski et al., 2024). To overcome these inaccuracies, watermasks have been used to help delineate where water courses are actually geolocated (Yamazaki et al., 2019), that is, editing the DEMs to force the correct representation of flow. Watermasks can be used to lower DEM elevations, ensure correct flow directions, and delineate waterways smaller than the DEM pixel size. However, existing global surface water extent data sets are inconsistent, with different data origins, data formats and definitions of surface water (Rajib et al., 2024). To minimize any negative impacts on hydrography delineation from migrating channels or other changing waterbodies, MERIT-Hydro used the G1WBM permanent water layer at 1-arc-sec spatial resolution which was considered the best water extent data set corresponding to the temporal period of the underlying DEM, MERIT DEM (Yamazaki et al., 2019).

Here, we use GRWL, as it aligns with the 2011–2015 acquisition period of Copernicus DEM (and thus FABDEM), and the ~30 m spatial resolution of FABDEM. Crucially, GRWL attempts to represent the extent of rivers globally at mean discharge by using Landsat imagery when those conditions are expected in each region. Furthermore, GRWL defines rivers in four classes: inland rivers, lakes, canals and coastal/tidal. To ensure a gap-less watermask, additional water surface products were blended with GRWL. The Global Surface Water Explorer (GSWE) (Pekel et al., 2016) occurrence raster data set was used to fill gaps between GRWL and the land-sea mask at river outlets. Finally, we filled any river islands smaller than a threshold of 1 km² and lake islands less than 50 km² to homogenize and generalize connectivity. This means bifurcations are only created to circumvent landmasses larger than these thresholds.

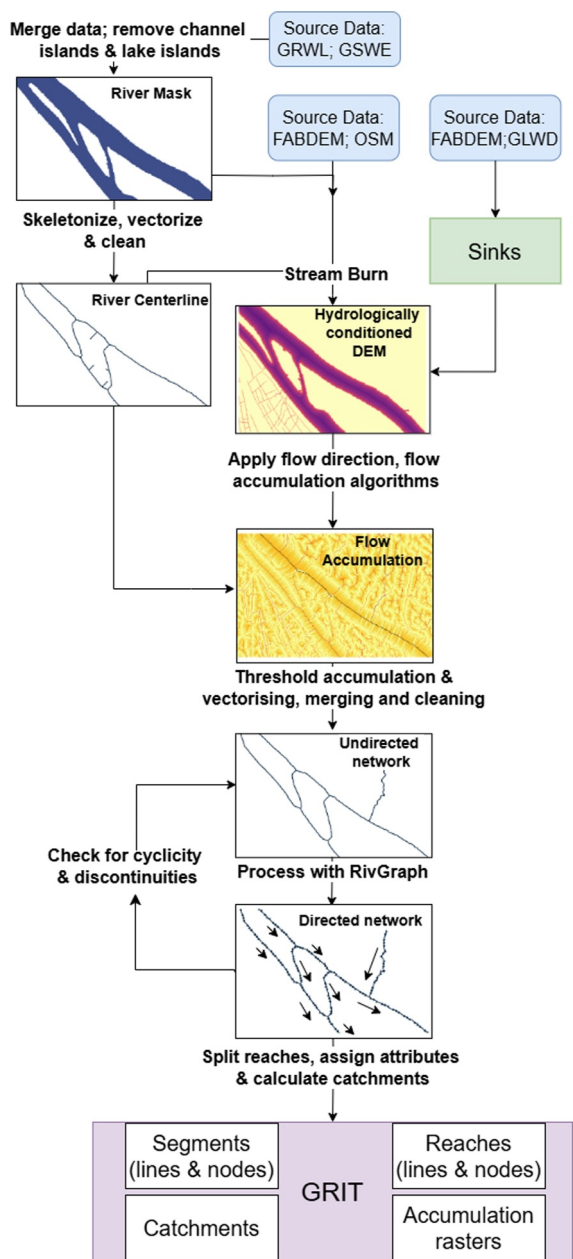


Figure 1. GRIT development workflow. The workflow of the river network creation includes inputs (blue boxes), processes (bold text), steps (graph/green boxes) and outputs (white boxes). Data set acronyms include Global River Widths from Landsat (GRWL), Global Surface Water Explorer (GSWE), OpenStreetMap (OSM), Forest And Buildings removed Copernicus DEM (FABDEM), Global Lakes and Wetlands Database (GLWD).

2.2. River Centerline Creation

We created a GRWL river centerline vector by skeletonizing the GRWL-based river mask (described in Section 2.1), reducing it to only the centerline pixels, and then vectorizing it. We employed basic topological cleaning to remove dangles (line segments that are only connected to the network at one end/node) and snapped line ends that were up to 120 m apart to enhance topological connectivity. Only these skeletonized centerlines were merged with the DEM-generated vector described in Section 2.5. Since the GRWL-based watermask can only delineate rivers above ~30 m resolution, owing to the resolution of the underlying Landsat data, we used water layers from OpenStreetMap (OSM) to produce an OSM river vector (alongside the GRWL river centerline vector) for streams below 30 m (Haklay & Weber, 2008). Despite completeness issues in OSM data, which are more prevalent in certain geographies, it remains an invaluable resource in delineating streams below 30 m resolution and has been used in other global hydrography data sets such as MERIT-Hydro (Yamazaki et al., 2019).

2.3. Sink Identification

Sinks are areas where the elevation is lower than the surrounding terrain, and thus have an undefined lateral flow direction with no outlet. In DEMs, sinks can be topographic depressions or flat areas (Lindsay, 2016) where flow would get incorrectly trapped when applying flow direction and accumulation algorithms. A key challenge in sink removal is to avoid the removal of real sinks that are not a product of inaccuracies in the DEM. We thus retained all sinks with a volume larger than a 20 km³ threshold (as a reference, this roughly corresponds to the volume of Lake Geneva), as a sink of this size would significantly influence the water balance of a river catchment. We selected this sink size to identify large, known sinks, while neglecting smaller, more uncertain ones that might not have a large-scale impact on the overall flow network. We acknowledge that this is larger than those used in MERIT-Hydro or HydroSHEDS, leading to greater connectivity in highly arid regions (see comparison in Figure S2 in Supporting Information S1).

To identify sinks, we used the GRASS add-on *r.hydrodem* function (Lindsay & Creed, 2005). The function first slightly denoises the input DEM by removing single cell peaks and pits, followed by filling sinks. The sink volume was calculated by finding the difference between the input DEM and sink filled DEM, clumping adjoining pixels, then summing up the volumes in each clump. Clumps exceeding the volume were reduced to their lowest 5% cells to define DEM-derived sinks. This was merged with endorheic lakes from the Global Lakes and Wetlands Database (GLWD; Lehner & Döll, 2004) and passed as sinks to the *r.watershed* module. Since the module finds the lowest outlet of leftover sinks in the DEM by default, the original values from FABDEM were used in Section 2.5. This preserves the flow paths from the DEM.

2.4. Hydrologically Conditioned DEM

A hydrologically conditioned (stream burned) DEM is required to represent correct flow paths over the landscape. After sink removal, some errors may remain in the DEM. Therefore, we further enhanced the hydrologically corrected DEM by using the GRWL and OSM derived river centerlines to lower DEM elevations by “burning” in the streams (i.e., “stream-burning”). Stream-burning is a commonly used approach to lower DEM elevations where rivers are located, thus ensuring flow over a landscape finds a river. Our approach is similar to the approach taken in MERIT-Hydro by choosing thresholds based on importance of the features. The lowering factor (LF) was defined as 10 m, roughly

corresponding to the higher end of the DEM uncertainty. We lower the GRWL-derived river centerlines by 5 LF and the distance to the banks within the GRWL river mask in cells by 2 LF. These values were selected by an iterative trial and error approach to ensure overlapping of the DEM-derived and skeletonized centerlines. By conditioning the elevation reduction by distance to the riverbank, we ensure a gentle gradient to the centerline, preventing parallel lines and artifacts on large, flat-water surfaces. Around centerline end nodes a 90 m buffer is applied with a LF of 3, which increases the likelihood that DEM-generated streams join up with ends of the GRWL centerline. OSM-derived centerlines were lowered by 2 LF for features with the OSM tag “waterway = river” or “waterway = canal” and 1 LF for any other feature that had the “waterway” tag defined. River width could not be used as an attribute to lower elevations for OSM data as width information was not available for most OSM rivers, nor could it be calculated with the absence of homogeneous OSM river polygons.

2.5. Accumulation and Drainage

Next, we generated flow direction maps, accumulation arrays and drainage areas based on the “traditional” hydrography generating algorithms used for previous, non-bifurcating hydrographies. We used the *r.watershed* module (Metz et al., 2011) in GRASS GIS due to its computational efficiency and performance using radar-based DEMs (Amatulli et al., 2022). In *r.watershed*, we used our hydrologically corrected DEM (see Section 2.4) and depression layer (see Section 2.3) as inputs. Flow directions were calculated using a single direction (D8) algorithm (O’Callaghan & Mark, 1984).

A single-threaded river network was delineated by extracting cells based on a drainage accumulation threshold of 50 km². This threshold was chosen to retain a suitable amount of complexity in the resultant river network, without creating an unwieldy data set that would be computationally challenging to process in the latter stages. Our threshold is higher than other hydrographies such as HydroRIVERS (Linke et al., 2019), which used a flow accumulation of 10 km², and Hydrography90 m (Amatulli et al., 2022), which used a flow accumulation of 0.05 km². As a result, the vector product may fail to depict some headwater areas which some geomorphology and ecohydrology applications may require. However, smaller headwaters can be inferred from the accumulation raster if needed. Finally, this rasterized delineation of a river network was vectorized to create a convergent network similar to the previous hydrographies.

2.6. Undirected Network

The single-threaded vector was merged with the GRWL centerlines vector described in Section 2.2. Because they were previously burned into the DEM, both vectors overlap inside the GRWL river mask and add the missing links that are absent from the DEM-derived network. Inside the GRWL river mask, the resultant network is undirected, as the GRWL centerline is undirected and the DEM-derived vector directions may be inconsistent with the actual flow directions in flat terrain.

Before the river network can be processed to create the directed network, it must be cleaned to remove erroneous lines and join disconnected parts of the network. Gaps between line ends of less than 120 m in the network (i.e., 4 GRWL pixels) were snapped together. Short segments that are only connected to the network at one end (dangles) or entirely disconnected segments were then removed, with different rules between rivers and lakes. In rivers, dangles less than two times the width derived from the underlying GRWL mask were removed. For lakes, we removed dangles less than 10 times the width. These thresholds were derived from trial and error. Erroneous loops caused by the vectorization were identified by first removing the longest line of the short loops and pruning the remaining dangles. Lastly, short dangles of less than 500 m were removed. This procedure was repeated iteratively to result in a clean network.

2.7. Directed Network

Within the clean river network, we then focused on establishing river network directionality using the RivGraph tool (Schwenk et al., 2020; Schwenk & Hariharan, 2021). RivGraph contains the functionality to assign flow directions to water masks of river deltas and sections of braided rivers. It uses a series of topological and heuristic direction-predicting algorithms. Flow directions are initially “guessed” based on these algorithms, and guesses are then used to assign flow directions in an iterative approach that works from the most certain network segments to the least certain. The most common algorithms assign flow directions by enforcing topological continuity (i.e., avoiding sources or sinks within the network) and avoiding cycles. Where multiple guesses disagree and

Table 1
A Brief Description of the Main GRIT Vector Data Sets

GRIT data set	Description
Network Segments	Lines and nodes between inlet, outlet, confluences and bifurcation nodes
Network Reaches	Lines and nodes of segments lines split to not exceed 1 km in length
Catchments	Catchment outlines for entire river basins (network components), segments and reaches

Note. See Wortmann et al. (2024) for sources. Raster products and vector attributes are listed in Tables S1–S7 in Supporting Information S1.

continuity or cycle prevention cannot assign the direction, the direction with most guesses is chosen. Different networks require different approaches or recipes given on the available direction predicting attributes. RivGraph provides well-tested recipes for river deltas and sections of braided rivers.

We extended RivGraph by using a width continuity algorithm, and gradients of accumulation, distance to outlets and elevation within a segment as additional direction predicting attributes. The width continuity algorithm assumes that river widths do not change significantly at bifurcations or confluences, that is, the combined widths of two tributaries/distributaries should be similar to the width of their downstream/upstream river. This assumption can be exploited to assign directions when one or two segments at a node are known but others are not. We assigned directions when the alternative node type would lead to a change in width by a factor outside of the range 1/5 to 5.

A RivGraph recipe was created to handle entire river networks using the RivGraph algorithms and direction-predicting attributes. As a starting point, inlet and outlet nodes were identified. Line ends in the ocean (identified using the OSM land-sea mask) or a sink (identified in Section 2.3) were considered as outlets, while all other single-line nodes were deemed inlets. All segments outside of the GRWL river mask were directed by their flow accumulation gradient. Single-threaded and large (flow accumulation > 1,000 km²) segments were also set by the flow accumulation gradient. Then, directions were set iteratively by progressively increasing the flow angle by 2° increments from the most shallow angle of 0° to a maximum flow direction change of 40°. Directions of remaining segments were successively assigned by agreement of direction-predicting attributes and finally by shortest path to an outlet. This recipe was optimized through trial and error using cyclicity and discontinuity as objective functions.

The handling of cyclic topology in the network was a unique challenge. To address this, topological cleaning was implemented to create directed, acyclic graphs (DAGs). RivGraph already includes functions to remove cyclicity. These functions typically unassign all flow directions in a cycle, then iteratively switch the flow direction of the most uncertain cycle segments, followed by a re-assignment of all other flow directions following the usual direction prediction algorithms. Most challenging were cycles that created sink catchments without ending in a sink, as they require a much larger search radius to find and resolve problematic segments. These cycles were resolved by resetting all upstream segments' directions, then finding the path to the nearest outlet from the cycle and re-running the entire recipe for the remaining unset ones. After this fully automated process, 74 cycles remained globally, whose segments were either removed if they only had neighboring segments leaving the cycle ($N = 44$) or resolved by manually assigning flow directions ($N = 30$).

2.8. Final Products

The final step was to assign attributes to the directed network and create ancillary products. A full description of the attributes in GRIT is provided in Tables S1–S7 in Supporting Information S1 and brief descriptions of data sets are given in Table 1. Some notable attributes are drainage area, Strahler orders and a main channel flag, as they are routinely used in river models and analyses. Two types of drainage area are provided: (a) Drainage areas were assigned to each segment “routing” the DEM-derived flow accumulation at inlets to the outlets. The process of flow partitioning at bifurcations was addressed by using width-based percentages to determine how drainage area is divided among the two channels. In the absence of in-situ vertical information, width was found to be the most predictive approach for flow partitioning (Dong et al., 2020). More complex partitioning schemes are enabled within GRIT by providing the incidence angles of segments and other attributes. (b) Similarly, a single-threaded drainage area is provided, that is, at bifurcations all drainage area is “routed” along the mainstems. The

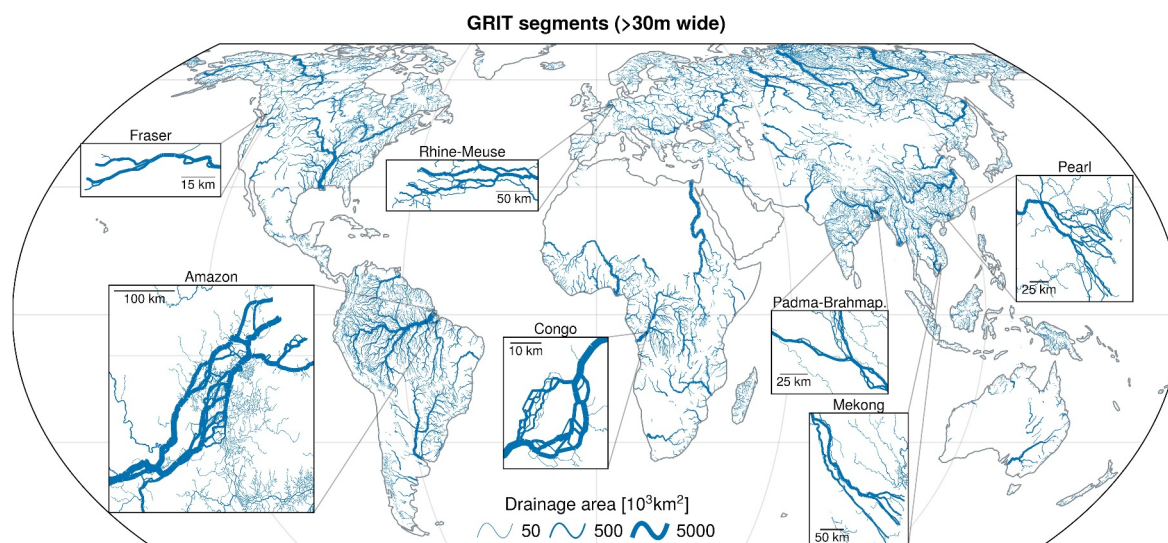


Figure 2. Global map of the GRIT network. The network is shown for all reaches with GRWL width greater than 30 m as well as their downstream segments. The width is scaled by partitioned drainage area here for visualization purposes. The inset maps show the multi-threaded river network at regional scale in seven selected regions of the globe (Fraser, Amazon, Rhine-Meuse, Congo, Padma-Brahmaputra, Mekong and Pearl Rivers). Line widths in inset panels have their own scale also reflective of drainage area rather than river width.

mainstems are determined by following the widest channel at bifurcations, which is typically indicative of the main flow path. Knowing the mainstems allows GRIT also to be used as a single-threaded network and highlights the secondary distributary channels that set GRIT apart from purely convergent hydrographies.

Since river-based tools, models and analyses are typically applied to shorter reaches of more uniform lengths, a river reach data set is also provided. The network segments are split into equally long parts between two nodes, each smaller than 1 km. These reaches were slightly straightened to remove the sharp zigzagging introduced by the underlying rasters and ensure a realistic approximation of the river's course, but the location of the nodes remains unchanged. Catchments for entire network components (all connected parts), for each segment and for each reach were delineated using the *r.stream.basins* GRASS GIS module (Jasiewicz & Metz, 2011).

Vector files are provided in GeoPackage format in both the original equal-area Equal Earth Greenwich projection (EPSG:8857) as well as in geographic WGS84 coordinates (EPSG:4326) and are freely available on Zenodo (Wortmann et al., 2024). To keep file sizes manageable, vector layers are split into seven regions, in addition to a simplified network covering the globe. The network files contain lines and nodes, with catchments available as polygons. Raster based products (flow accumulation, flow direction, height above and distance from nearest drainage at 30 m resolution, see Table S1 in Supporting Information S1) are also available upon request.

3. Results and Network Evaluation

3.1. Overview of GRIT

The GRIT network consists of 30 m raster layers (such as flow accumulation, drainage direction, catchments and other derivatives; see Table S1 in Supporting Information S1) and vector maps (such as river segments, reaches, nodes and catchments; see Table S2 in Supporting Information S1). The vector maps focus on streams and rivers with drainage areas greater than 50 km² and include topological and morphological attributes derived from the underlying 30 m raster maps. This global vector network has a total length of 19.6 million km over 1.76 million network segments that are connecting 788,823 inlets, 818,437 confluences, 67,495 bifurcations and 31,528 outlets (6,533 of those in sinks). Rivers wider than 30 m (Figure 2), that is, those primarily delineated from the GRWL river mask enabling bifurcations, have a length of 2.87 million km.

GRIT's representation of multi-threaded rivers is the first global data set of river bifurcations (Figure 3). The total number of bifurcations identified in GRIT reaches is c.65,000, located mostly in rivers but also in coastal areas.

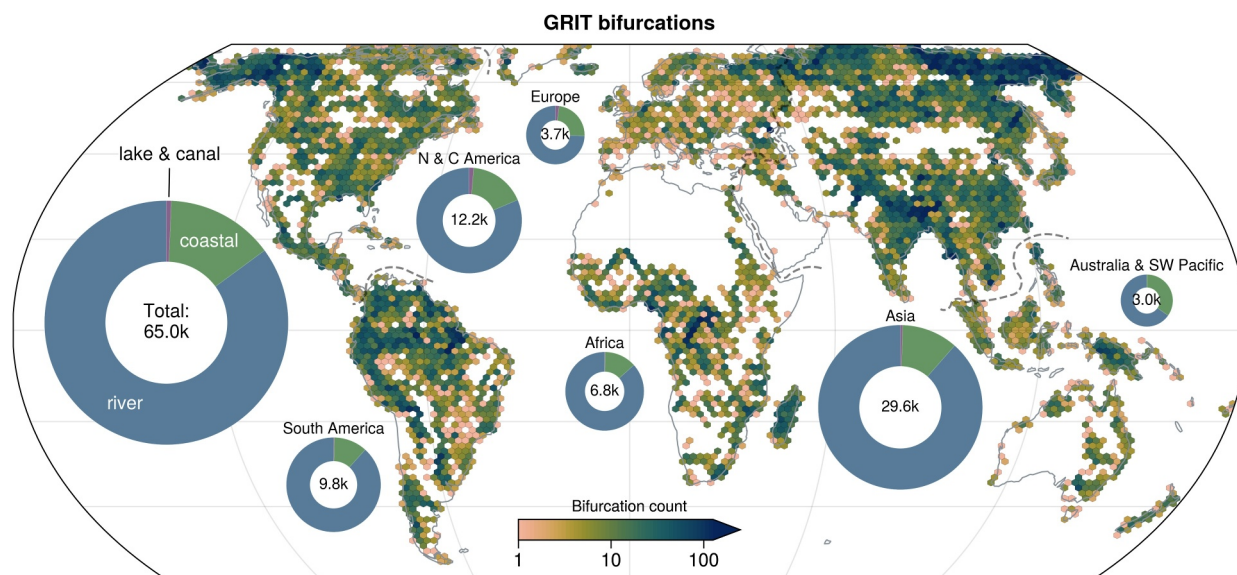


Figure 3. Distribution of river bifurcations, including global and continental totals. Doughnuts indicate the GRWL classification. Yellow-to-blue color gradient indicates the total number of bifurcations within each hex bin. The share of bifurcations located along rivers, coastal areas or lakes and canals is indicated within each donut, for each continent.

The largest number of bifurcations is found in Asia (c.29,600), followed by North and Central America (c.12,200) and South America (c.9,800).

3.2. Visual Comparison Between GRIT and Existing Networks (MERIT-Hydro and HydroSHEDS)

The advancement of GRIT over currently available hydrographies is most evident at the local scale (Figure 4 and Figure S1 in Supporting Information S1). First, the change in resolution from 90 to 30 m, based on the FABDEM DEM, allows for a more precise representation of various river network features. This can be seen, for example, in the greater detail on river locations and longitudinal variability (i.e., meanders). Second, the centerlines of rivers greater than 30 m are at the center of the river mask, which is not guaranteed in purely DEM-generated hydrographies. Third and most strikingly, GRIT represents divergent flow paths and partitions flow at bifurcations. These links are absent from MERIT-Hydro and HydroSHEDS, leading to overestimations of flow in the primary reach and an underestimation or omission of flow in the secondary reach downstream of bifurcations when routing flow. Although GRIT includes bifurcations, data on the mainstems and a single threaded network are also provided. This dual focus is essential for comprehensive river network analysis, as it captures both the complexity of river systems and the dominance of main channels. Future work could compare the different existing river networks against maps of time-integrated Global Surface Water Occurrence (Pekel et al., 2016).

GRIT also includes canals that are larger than 30 m wide, which is a significant addition over some existing hydrographic networks. This capability is particularly beneficial for areas where canals play a major role in the water network. A unique feature of GRIT is its use of multispectral imagery to infer the centerline of rivers. This approach means that the GRIT network can be easily updated. This ability for GRIT to be updated is particularly valuable for monitoring and modeling dynamic river systems, which can change substantially over time due to natural processes and human activities.

3.3. Evaluation of Gauge Snapping Distance

GRIT's validation process involved a suite of methods to ensure the accuracy of the river network. Gauging stations play a significant role in this validation process. We assess the snapping distance of the network to the gauging stations and compare the reported drainage areas where the gauge has snapped to the network. Stations are first snapped to the nearest point on the network and if that led to a drainage area deviation of more than 20%, snapping is then repeated to parts of the network that are within $\pm 20\%$ of the station's reported drainage area. Compared with the MERIT-Hydro and HydroSHEDS networks, we find marginal differences in gauge snapping

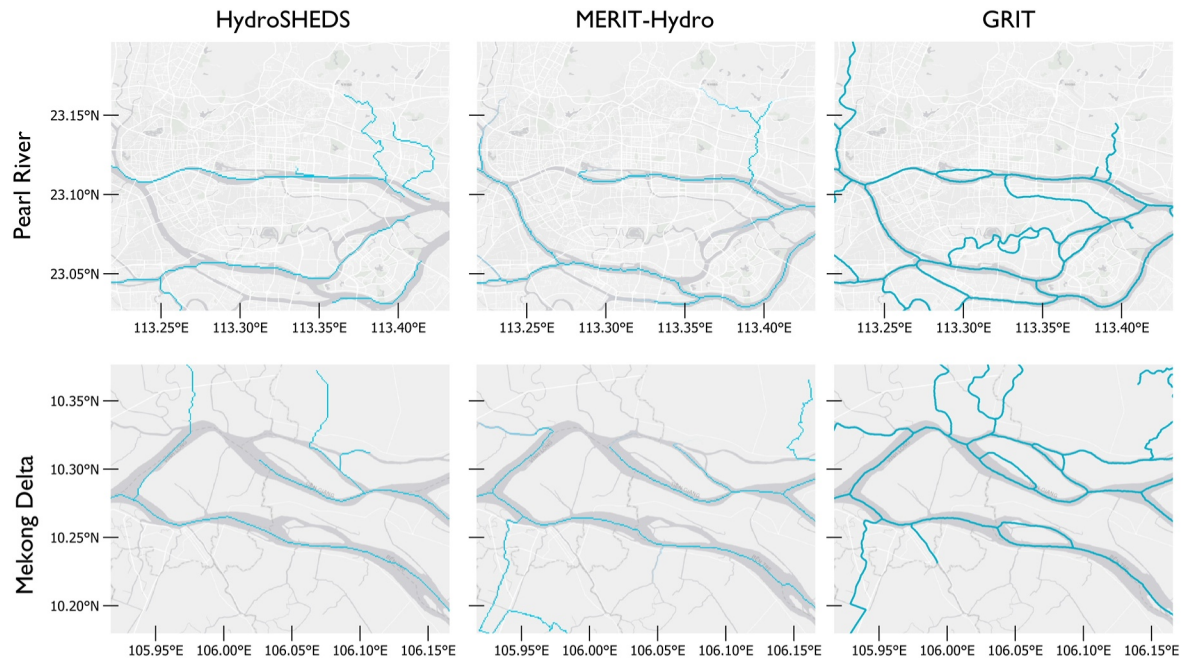


Figure 4. A comparison of GRIT with MERIT-Hydro and HydroSHEDS. Center lines are shown in blue in HydroSHEDS (90 m; left column); MERIT-Hydro (90 m; middle column); and GRIT (30 m; right column). Two locations are shown: Guangzhou in the Pearl River delta, southern China, approx. 50 km upstream of the mouth (top row), and the Mekong delta (bottom row). The same drainage area threshold is shown in all three networks for consistency. The minimum drainage accumulation threshold is 50 km² in line with the minimum drainage accumulation used in GRIT.

(Figure 5). We have also compared the distributed drainage area between GRIT and the two hydrographs for rivers larger than 1000 km² within the 5 × 5 arcmin search window (see Figure S2 in Supporting Information S1). This revealed mainly the differences in the sink thresholds, that is, GRIT includes fewer sinks in arid regions than the other hydrographs. Outside of arid regions, drainage areas only show small deviations, with isolated exceptions where either the routing of GRIT is different or the river mainstems do not align within the search

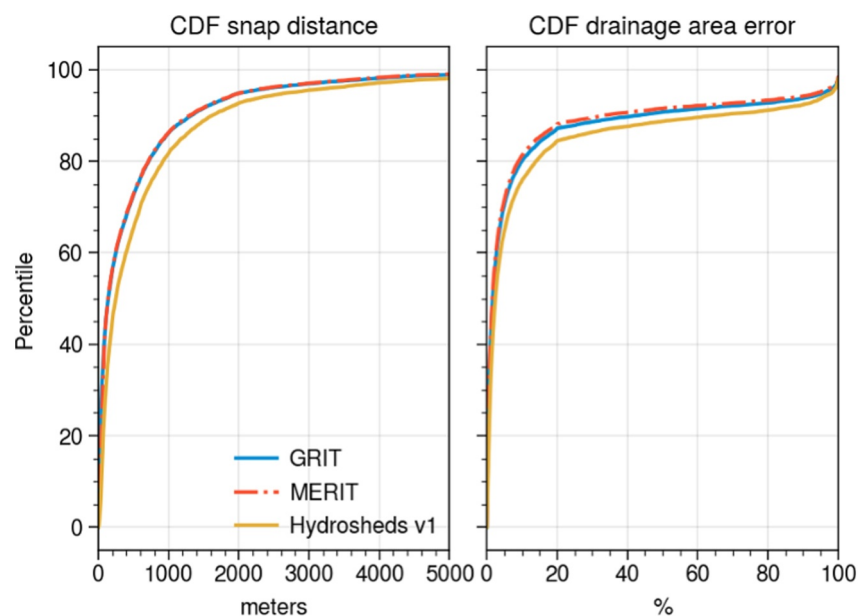


Figure 5. Cumulative density function comparing the gauge snapping distance (left panel) and drainage area error (right panel) in the GRIT network (blue line) with those of the MERIT (red dashed line) and HydroSHEDS (orange line) networks.

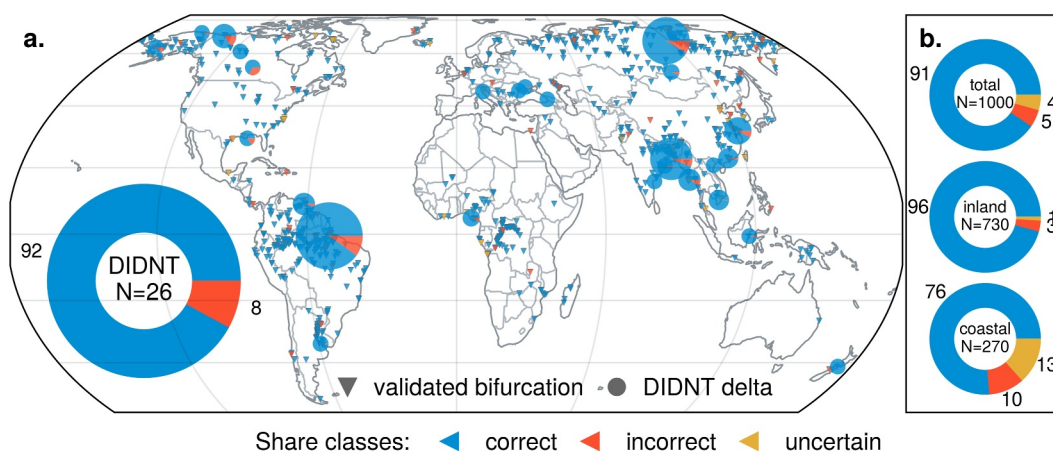


Figure 6. Validation of delta network directions and bifurcations in GRIT. (a) Delta network directions from the Discharge In Distributary NeTworks (DIDNT) network matched by GRIT; circles on the map are DIDNT locations. (b) Manual checking of bifurcation points broken down by all areas, inland and coastal; triangles are validated bifurcation points. Blue indicates proportion of matches, orange proportion of misses (different directions), and yellow indicates “impossible to tell” (bifurcation points only). The numbers associated with the doughnut graphs represent the proportion as a percentage.

window, for example, in deltas. It is worth noting that both MERIT and HydroSHEDS have been manually edited, contrary to GRIT, which is largely automated to improve reproducibility and enable updates.

3.4. Evaluation of Bifurcation Points

Our approach for validation includes a thorough randomized check of flow directions in the distributary network components. We randomly selected 1000 locations representing the full distribution of catchment areas to assess the quality of the distributary network (see Supporting Information S1). For each location, we used high-resolution satellite imagery to determine the flow direction, providing a real-world comparison to the network. We assessed each of the 1,000 bifurcation points against three criteria: (a) correct bifurcation; (b) incorrect bifurcation (e.g., should be a confluence); (c) impossible to tell (e.g., areas located in the coastal zone, where the water could be flowing in both directions). A full description of the bifurcation validation procedure is provided in the Text S1 and Figures S3–S5 in Supporting Information S1. As a benchmark, we employed the GRWL river mask on which GRIT is based. Results, shown in Figure 6b, indicate that 91% of GRIT's bifurcation points were correct. There were very few incorrect bifurcation points within the fluvial part of the network, with 96% matching, 1% uncertain and just 3% incorrect (out of 730 bifurcation points). Coastal areas had a smaller proportion of correct bifurcation points, with a 76% correct rate and 10% incorrect.

3.5. Comparison to the Discharge In Distributary NeTworks (DIDNT) Data Set

The Discharge In Distributary NeTworks (DIDNT) data set (Hariharan et al., 2022) contains networks and discharge partitioning estimates for 28 deltas globally, calculated using RivGraph. We compare GRIT against the DIDNT data set as it includes high quality, manually corrected delta networks that are similar to GRIT, but derived from 10 m river masks. To compare, we snapped segments from DIDNT to GRIT reaches and calculated the azimuth difference. Figure 6 shows the proportion of GRIT river segments that matched the DIDNT river network. Segments are deemed invalid if the DIDNT segments that were snapped are further than their corresponding river width away. Similarly, segments that have an average width narrower than 30 m, or are near-perpendicular to the snapped GRIT segment (azimuth differences between 75 and 105°), are also deemed invalid. In contrast, segments are deemed correct if they are not invalid and have azimuth differences below 75°. Segments are considered incorrect if they are not invalid but have azimuth differences above 105°. This approach allows for a detailed assessment of GRIT's accuracy and the identification of areas that may need refinement. We identified 92% match of directions between GRIT and DIDNT globally. Across the 28 deltas, matches are typically above 90% (Figure 6a) for most locations. Given that the DIDNT network represents some of the most

complex parts of the global river network, this performance is likely to be a conservative measure of GRIT's overall accuracy.

4. Discussion: Implications and Limitations

4.1. Impact of GRIT for Global Assessments

The impact of GRIT for global assessments may be significant, particularly for global flood analyses and large-scale hydrological modeling. For global flood analyses, GRIT offers a more detailed and accurate representation of river networks. GRIT's high resolution and precise depiction of river courses, including bifurcations and accurate channel positions, can be used to enhance the accuracy of flood risk assessments and predictions. For example, large-scale flood models routinely use drainage area to derive river bathymetry. GRIT provides this also for distributaries and hence is directly transferable to these models that have previously been used only in single deltas (Ikeuchi et al., 2015; Yamazaki et al., 2014). This improved accuracy will be valuable for better understanding of flood hazard at the global scale.

In the realm of large-scale and global hydrological modeling, there is a clear trend toward hyper-resolution modeling (Bierkens, 2015; Wood et al., 2011). GRIT aligns with this trend, offering a higher resolution and more detailed river hydrography to support these advanced modeling efforts and the use of data-driven models based on artificial intelligence and machine learning (AI/ML). By providing more granular information, GRIT enables a more nuanced understanding of hydrological processes at smaller scales, which is essential for addressing the complexities of global water systems.

A last key aspect of GRIT is its vector-based approach that harnesses the value of river masks, which can be generated from a variety of sources. Previous global networks relied mainly on DEMs, and were inherently raster-based approaches, where the topology and linear characteristics of streams and rivers were often secondary considerations. The vector-based approach of GRIT shifts the focus, allowing for more detailed topological investigations and representations of river networks. This shift opens up new opportunities for exploring and understanding the intricate patterns and behaviors of global water systems, leading to more comprehensive and effective water management strategies on a global scale. A significant advantage over the DEM-only approach is also the ability to update GRIT with improved or up-to-date river masks from various Earth Observation data sets, without the need for improved/costly elevation data.

4.2. Limitations and Possible Future Improvements

As with any new approach, GRIT has challenges and areas for possible future improvements. A primary area for potential improvement is consideration of the semi-permanence of the river network, including bifurcations and distributaries. River channels and deltas can change over time due to natural and human causes, with some bifurcations and distributaries being temporary or fluctuating with seasonal or environmental changes. A deeper understanding of this phenomenon is necessary for accurately modeling river networks, as it affects the representation of river flow and the dynamics of river systems. The ability to update the GRIT river network with improved river masks from Earth Observation data sets is one of GRIT's strengths and brings us closer to addressing the nonstationarity in river systems. In the future, GRIT could be enhanced to function as a dynamically updating river network. This could be accomplished by identifying portions of the river network that bifurcate or change seasonally, such as the Brahmaputra, updating such locations at regular intervals, and connecting them to a more stationary meta layer. Another key issue in GRIT is related to vectorization. Specifically, there are discontinuities in the GRWL mask that stem from its 30 m resolution. Currently these discontinuities are addressed by GRIT's approach to filling gaps using single flow directions, but this approach could be improved, as discontinuities can lead to inaccuracies in representing the complex network of river channels, particularly in areas where rivers split into multiple channels or merge. A higher resolution river mask would fill these discontinuities, as smaller channels would be included. Human-made diversions wider than 30 m are currently represented in GRIT, but any smaller diversions would also require a higher-resolution river mask or other globally consistent data sets representing these flow paths, which for example, OSM currently does not provide.

It is also important to note that although GRIT is burning in river centerlines from OSM outside of the GRWL river mask, flow lines may not always correspond to observed river flow and thus may not always agree with the

location of the water table, as is required for for example, groundwater models. Within the GRWL river mask, centerlines are always true to the Landsat/GRWL observations.

Overall, addressing these limitations and implementing suggested improvements would enhance GRIT's reliability and accuracy in future iterations. With the advent of hyper-resolution modeling and AI/ML, GRIT is expected to greatly improve the accuracy of many river-based applications such as flood forecasting, water availability and quality simulations, or riverine habitat mapping. For instance, machine learning models can be trained to predict hydrologically relevant variables such as the bankfull river channel conveyance capacity (Liu et al., 2024) and then produce globally distributed estimates along the GRIT network. This approach can be used to develop essential input data sets for Global Flood Models or to enhance ML-based hydrological forecasting.

5. Conclusions

In this research we sought to address a significant gap in the representation of global river networks, namely the mapping of river bifurcations, multi-threaded rivers, deltas, and artificial channels. Recognizing the limitations of existing elevation-derived networks such as HydroSheds and MERIT Hydro, which largely ignore these complex features, our goal was to develop a more comprehensive and accurate global river network. To achieve this, we employed a novel approach, combining a 30 m Landsat-based river mask with elevation-generated streams, and integrating a more accurate 30 m digital terrain model (FABDEM) in place of traditional SRTM derivatives. This vector-based approach not only captures the tributary components but also the distributary components of river networks, including intricate multi-threaded channels, canals, and delta distributaries.

GRIT offers a significant improvement for the accuracy of river-based geoscience and machine learning applications, ranging from flood modeling and forecasting to water quality simulations and riverine habitat mapping. The inclusion of features like multi-threaded rivers and bifurcations ensures that GRIT is more reflective of the real-world complexities of river systems, particularly in densely populated and ecologically critical areas such as large river deltas. However, GRIT does have limitations, including challenges in vectorization or inaccurate directions in highly complex, multi-threaded parts of the network. These aspects highlight areas for further research, such as improving vector-based representation and exploring alternative methods for handling complex river systems. Further development and refinement of GRIT will be crucial in advancing our understanding and management of global water systems, especially as the field moves toward hyper-resolution modeling in hydrology, ecology, and related disciplines.

Conflict of Interest

The authors declare no conflicts of interest relevant to this study.

Data Availability Statement

The GRIT network is made available on Zenodo (Wortmann et al., 2024). The vector data sets are split by data set and region, named *GRITv<version>_<dataset>_<region>_<crs>.gpkg.zip* in the *Files* section. The code to produce the GRIT data sets is published as Wortmann (2025). This work builds on several publicly available data sets, including the Global River Width from Landsat (GRWL) raster river mask (Allen & Pavelsky, 2018a); the 30 m FABDEM (Hawker & Neal, 2021); the Global Surface Water Explorer (GSWE) raster data set (Pekel et al., 2016) and the Global Lakes, reservoirs and Wetlands Database (GLWD; Lehner & Döll, 2004). The GRIT data sets produced are listed in Table 1, with details in Tables S1–S7 in Supporting Information S1.

Acknowledgments

This work is part of the Evolution of Global Flood Hazard and Risk (EvoFlood) project supported by the Natural Environment Research Council supporting MW/YL/LS (NE/S015728/1), LH/JN (NE/S015639/1), PA (NE/S015655/1), RB/GSS (NE/S015736/1), HC/HG (NE/S015590/1), PD/SJM/DP (NE/S015795/2), SHG/JL/SED (NE/S015817/1), and APN/EV (NE/S015612/1). LS was additionally supported by UKRI (MR/V022008/1). We thank Dai Yamazaki, David Blodgett and the Editors for their insightful suggestions which improved the quality of the manuscript.

References

- Alfieri, L., Salamon, P., Bianchi, A., Neal, J., Bates, P., & Feyen, L. (2014). Advances in pan-European flood hazard mapping. *Hydrological Processes*, 28(13), 4067–4077. <https://doi.org/10.1002/hyp.9947>
- Allen, G. H., & Pavelsky, T. M. (2018a). Global River Widths from Landsat (GRWL) database [Dataset]. <https://doi.org/10.5281/zenodo.1297434>
- Allen, G. H., & Pavelsky, T. M. (2018b). Global extent of rivers and streams. *Science*, 361(6402), 585–588. <https://doi.org/10.1126/science.aat0636>
- Altenau, E. H., Pavelsky, T. M., Durand, M. T., Yang, X., Frasson, R. P. D. M., & Bendezu, L. (2021a). The Surface Water and Ocean Topography (SWOT) Mission River Database (SWORD): A global river network for satellite data products. *Water Resources Research*, 57(7), e2021WR030054. <https://doi.org/10.1029/2021WR030054>
- Altenau, E. H., Pavelsky, T. M., Durand, M. T., Yang, X., Frasson, R. P. D. M., & Bendezu, L. (2021b). SWOT River Database (SWORD). <https://doi.org/10.5281/zenodo.3898570>

- Amatulli, G., Garcia Marquez, J., Sethi, T., Kiesel, J., Grigoropoulou, A., Üblacker, M., et al. (2022). Hydrography90m: A new high-resolution global hydrographic dataset. *Earth System Science Data Discussions*, 2022(10), 1–43. <https://doi.org/10.5194/essd-14-4525-2022>
- Bielski, C., López-Vázquez, C., Grohmann, C. H., Guth, P. L., Hawker, L., Gesch, D., et al. (2024). Novel approach for ranking DEMs: Copernicus DEM improves one arc second open global topography. In *IEEE transactions on geoscience and remote sensing* (Vol. 62, pp. 1–22). <https://doi.org/10.1109/TGRS.2024.3368015>
- Bierkens, M. F. (2015). Global hydrology 2015: State, trends, and directions. *Water Resources Research*, 51(7), 4923–4947. <https://doi.org/10.1002/2015WR017173>
- Bierkens, M. F., Bell, V. A., Burek, P., Chaney, N., Condon, L. E., David, C. H., et al. (2015). Hyper-resolution global hydrological modelling: What is next? “Everywhere and locally relevant”. *Hydrological Processes*, 29(2), 310–320. <https://doi.org/10.1002/hyp.10391>
- Carlson, K. A., Levin, H. K., Morris, A. L., Candela, S. G., Rivera, A. M. M., Huening, V. G., & Fredericks, J. G. (2024). TDX-Hydro: Global high-resolution hydrography derived from TanDEM-X. <https://doi.org/10.22541/essoar.171629686.65893579/v1>
- Chen, X., Yu, M., Liu, C., Wang, R., Zha, W., & Tian, H. (2022). Topological and dynamic complexity of the Pearl River Delta and its responses to human intervention. *Journal of Hydrology*, 608, 127619. <https://doi.org/10.1016/j.jhydrol.2022.127619>
- Coffey, T. S., & Shaw, J. B. (2017). Congruent bifurcation angles in river delta and tributary channel networks. *Geophysical Research Letters*, 44(22), 11–427. <https://doi.org/10.1002/2017GL074873>
- Cohen, S., Kettner, A. J., Syvitski, J. P., & Fekete, B. M. (2013). WBMsd, a distributed global-scale riverine sediment flux model: Model description and validation. *Computers & Geosciences*, 53, 80–93. <https://doi.org/10.1016/j.cageo.2011.08.011>
- David, C. H., Maidment, D. R., Niu, G. Y., Yang, Z. L., Habets, F., & Eijkhout, V. (2011). River network routing on the NHDPlus dataset. *Journal of Hydrometeorology*, 12(5), 913–934. <https://doi.org/10.1175/2011JHM1345.1>
- Dong, T. Y., Nittrouer, J. A., McElroy, B., Illicheva, E., Pavlov, M., Ma, H., et al. (2020). Predicting water and sediment partitioning in a delta channel network under varying discharge conditions. *Water Resources Research*, 56(11), e2020WR027199. <https://doi.org/10.1029/2020WR027199>
- Doocy, S., Daniels, A., Murray, S., & Kirsch, T. D. (2013). The human impact of floods: A historical review of events 1980–2009 and systematic literature review. *PLoS currents*, 5. <https://doi.org/10.1371/currents.dis.f4deb457904936b07c09daa98ee8171a>
- Dottori, F., Szewczyk, W., Ciscar, J. C., Zhao, F., Alfieri, L., Hirabayashi, Y., et al. (2018). Increased human and economic losses from river flooding with anthropogenic warming. *Nature Climate Change*, 8(9), 781–786. <https://doi.org/10.1038/s41558-018-0257-z>
- Fatichi, S., Ivanov, V. Y., Paschalis, A., Peleg, N., Molnar, P., Rinkus, S., et al. (2016). Uncertainty partition challenges the predictability of vital details of climate change. *Earth's Future*, 4(5), 240–251. <https://doi.org/10.1002/2015EF000336>
- Gebrechorkos, S. H., Leyland, J., Dadson, S. J., Cohen, S., Slater, L., Wortmann, M., et al. (2024). Global scale evaluation of precipitation datasets for hydrological modelling. *Hydrology and Earth System Sciences*, 28(14), 3099–3118. <https://doi.org/10.5194/hess-28-3099-2024>
- Gosling, S. N., Zaherpour, J., Mount, N. J., Hattermann, F. F., Dankers, R., Arheimer, B., et al. (2017). A comparison of changes in river runoff from multiple global and catchment-scale hydrological models under global warming scenarios of 1°C, 2°C and 3°C. *Climatic Change*, 141(3), 577–595. <https://doi.org/10.1007/s10584-016-1773-3>
- Haklay, M., & Weber, P. (2008). Openstreetmap: User-generated street maps. *IEEE Pervasive computing*, 7(4), 12–18. <https://doi.org/10.1109/MPRV.2008.80>
- Hariharan, J., Piliouras, A., Schwenk, J., & Passalacqua, P. (2022). Width-based discharge partitioning in distributary networks: How right we are. *Geophysical Research Letters*, 49(14), e2022GL097897. <https://doi.org/10.1029/2022GL097897>
- Hawker, L., & Neal, J. (2021). Fdbdem v1-0 [Dataset]. <https://doi.org/10.5523/bris.25wfy0f9ukoge2gs7a5mqpq2j7>
- Hawker, L., Uhe, P., Paulo, L., Sosa, J., Savage, J., Sampson, C., & Neal, J. (2022). A 30 m global map of elevation with forests and buildings removed. *Environmental Research Letters*, 17(2), 024016. <https://doi.org/10.1088/1748-9326/ac4d4f>
- Hirabayashi, Y., Mahendran, R., Koirala, S., Konoshima, L., Yamazaki, D., Watanabe, S., et al. (2013). Global flood risk under climate change. *Nature Climate Change*, 3(9), 816–821. <https://doi.org/10.1038/nclimate1911>
- Ikeuchi, H., Hirabayashi, Y., Yamazaki, D., Kiguchi, M., Koirala, S., Nagano, T., et al. (2015). Modeling complex flow dynamics of fluvial floods exacerbated by sea level rise in the Ganges–Brahmaputra–Meghna Delta. *Environmental Research Letters*, 10(12), 124011. <https://doi.org/10.1088/1748-9326/10/12/124011>
- Jasiewicz, J., & Metz, M. (2011). A new GRASS GIS toolkit for Hortonian analysis of drainage networks. *Computers & Geosciences*, 37(8), 1162–1173. <https://doi.org/10.1016/j.cageo.2011.03.003>
- Jerolmack, D. J., & Swenson, J. B. (2007). Scaling relationships and evolution of distributary networks on wave-influenced deltas. *Geophysical Research Letters*, 34(23), L23402. <https://doi.org/10.1029/2007GL031823>
- Lehner, B., & Döll, P. (2004). Development and validation of a global database of lakes, reservoirs and wetlands. *Journal of Hydrology*, 296(1–4), 1–22. <https://doi.org/10.1016/j.jhydrol.2004.03.028>
- Lehner, B., & Grill, G. (2013). Global river hydrography and network routing: Baseline data and new approaches to study the world's large river systems. *Hydrological Processes*, 27(15), 2171–2186. <https://doi.org/10.1002/hyp.9740>
- Lehner, B., Verdin, K., & Jarvis, A. (2008). New global hydrography derived from spaceborne elevation data. *Eos, Transactions American Geophysical Union*, 89(10), 93–94. <https://doi.org/10.1029/2008EO100001>
- Lin, P., Pan, M., Beck, H. E., Yang, Y., Yamazaki, D., Frasson, R., et al. (2019). Global reconstruction of naturalized river flows at 2.94 million reaches. *Water Resources Research*, 55(8), 6499–6516. <https://doi.org/10.1029/2019WR025287>
- Lin, P., Pan, M., Wood, E. F., Yamazaki, D., & Allen, G. H. (2021). A new vector-based global river network dataset accounting for variable drainage density. *Scientific Data*, 8(1), 28. <https://doi.org/10.1038/s41597-021-00819-9>
- Lindsay, J. B. (2016). Efficient hybrid breaching-filling sink removal methods for flow path enforcement in digital elevation models. *Hydrological Processes*, 30(6), 846–857. <https://doi.org/10.1002/hyp.10648>
- Lindsay, J. B., & Creed, I. F. (2005). Removal of artifact depressions from digital elevation models: Towards a minimum impact approach. *Hydrological Processes: An International Journal*, 19(16), 3113–3126. <https://doi.org/10.1002/hyp.5835>
- Linke, S., Lehner, B., Ouellet Dallaire, C., Ariwi, J., Grill, G., Anand, M., et al. (2019). Global hydro-environmental sub-basin and river reach characteristics at high spatial resolution. *Scientific Data*, 6(1), 283. <https://doi.org/10.1038/s41597-019-0300-6>
- Liu, C., Liu, W. S., Huot, H., Guo, M. N., Zhu, S. C., Zheng, H. X., et al. (2022). Biogeochemical cycles of nutrients, rare Earth elements (REEs) and Al in soil-plant system in ion-adsorption REE mine tailings remediated with amendment and ramie (*Boehmeria nivea* L.). *Science of the Total Environment*, 809, 152075. <https://doi.org/10.1016/j.scitotenv.2021.152075>
- Liu, Y., Wortmann, M., Hawker, L., Neal, J., Yin, J., Santos, M. S., et al. (2024). Global Estimation of river bankfull discharge reveals distinct flood recurrences across different climate zones. 22 October 2024, Preprint available at Research Square. <https://doi.org/10.21203/rs.3.rs-5185659/v1>

- Marsh, C. B., Harder, P., & Pomeroy, J. W. (2023). Validation of FABDEM, a global bare-Earth elevation model, against UAV-lidar derived elevation in a complex forested mountain catchment. *Environmental Research Communications*, 5(3), 031009. <https://doi.org/10.1088/2515-7620/acc56d>
- Meadows, M., Jones, S., & Reinke, K. (2024). Vertical accuracy assessment of freely available global DEMs (FABDEM, Copernicus DEM, NASADEM, AW3D30 and SRTM) in flood-prone environments. *International Journal of Digital Earth*, 17(1), 2308734. <https://doi.org/10.1080/17538947.2024.2308734>
- Metz, M., Mitasova, H., & Harmon, R. S. (2011). Efficient extraction of drainage networks from massive, radar-based elevation models with least cost path search. *Hydrology and Earth System Sciences*, 15(2), 667–678. <https://doi.org/10.5194/hess-15-667-2011>
- Moore, R. B., McKay, L. D., Rea, A. H., Bondelid, T. R., Price, C. V., Dewald, T. G., & Johnston, C. M. (2019). User's guide for the national hydrography dataset plus (NHDPlus) high resolution (No. 2019-1096). *US Geological Survey*. <https://doi.org/10.3133/ofr20191096>
- O'Callaghan, J. F., & Mark, D. M. (1984). The extraction of drainage networks from digital elevation data. *Computer Vision, Graphics, and Image Processing*, 28(3), 323–344. [https://doi.org/10.1016/s0734-189x\(84\)80011-0](https://doi.org/10.1016/s0734-189x(84)80011-0)
- Ordnance Survey. (2022). MasterMap networks—Water layer. Retrieved from <https://www.ordnancesurvey.co.uk/products/os-mastermap-networks-water-layer>
- Pekel, J. F., Cottam, A., Gorelick, N., & Belward, A. S. (2016). High-resolution mapping of global surface water and its long-term changes. *Nature*, 540(7633), 418–422. <https://doi.org/10.1038/nature20584>
- Rajib, A., Khare, A., Golden, H. E., Gupta, B. C., Wu, Q., Lane, C. R., et al. (2024). A call for consistency and integration in global surface water estimates. *Environmental Research Letters*, 19(2), 021002. <https://doi.org/10.1088/1748-9326/ad1722>
- Raymond, P. A., Hartmann, J., Lauerwald, R., Sobek, S., McDonald, C., Hoover, M., et al. (2013). Global carbon dioxide emissions from inland waters. *Nature*, 503(7476), 355–359. <https://doi.org/10.1038/nature12760>
- Rodríguez, E., Morris, C. S., & Belz, J. E. (2006). A global assessment of the SRTM performance. *Photogrammetric Engineering & Remote Sensing*, 72(3), 249–260. <https://doi.org/10.14358/PERS.72.3.249>
- Schwenk, J., & Hariharan, J. (2021). RivGraph: Automatic extraction and analysis of river and delta channel network topology. *Journal of Open Source Software*, 6(59), 2952. <https://doi.org/10.21105/joss.02952>
- Schwenk, J., Piliouras, A., & Rowland, J. C. (2020). Determining flow directions in river channel networks using planform morphology and topology. *Earth Surface Dynamics*, 8(1), 87–102. <https://doi.org/10.5194/esurf-8-87-2020>
- USGS. (2001). National Hydrography Dataset (NHD). <https://doi.org/10.3133/70046927>
- Wood, E. F., Roundy, J. K., Troy, T. J., Van Beek, L. P. H., Bierkens, M. F., Blyth, E., et al. (2011). Hyperresolution global land surface modeling: Meeting a grand challenge for monitoring Earth's terrestrial water. *Water Resources Research*, 47(5). <https://doi.org/10.1029/2010WR010090>
- Wortmann, M. (2025). Global River Topology (GRIT) code, version 0.6 [Code]. *Zenodo*. <https://doi.org/10.5281/zenodo.14697233>
- Wortmann, M., Slater, L., Hawker, L., Liu, Y., & Neal, J. (2024). Global River Topology (GRIT), version 0.6 [Dataset]. *Zenodo*. <https://doi.org/10.5281/zenodo.7629907>
- Yamazaki, D., Ikeshima, D., Sosa, J., Bates, P. D., Allen, G. H., & Pavelsky, T. M. (2019). MERIT hydro: A high-resolution global hydrography map based on latest topography dataset. *Water Resources Research*, 55(6), 5053–5073. <https://doi.org/10.1029/2019WR024873>
- Yamazaki, D., Ikeshima, D., Tawatari, R., Yamaguchi, T., O'Loughlin, F., Neal, J. C., et al. (2017). A high-accuracy map of global terrain elevations. *Geophysical Research Letters*, 44(11), 5844–5853. <https://doi.org/10.1002/2017GL072874>
- Yamazaki, D., Kanae, S., Kim, H., & Oki, T. (2011). A physically based description of floodplain inundation dynamics in a global river routing model. *Water Resources Research*, 47(4), W04501. <https://doi.org/10.1029/2010WR009726>
- Yamazaki, D., Sato, T., Kanae, S., Hirabayashi, Y., & Bates, P. D. (2014). Regional flood dynamics in a bifurcating mega delta simulated in a global river model. *Geophysical Research Letters*, 41(9), 3127–3135. <https://doi.org/10.1002/2014GL059744>
- Yan, D., Wang, K., Qin, T., Weng, B., Wang, H., Bi, W., et al. (2019). A data set of global river networks and corresponding water resources zones divisions. *Scientific Data*, 6(1), 219. <https://doi.org/10.1038/s41597-019-0243-y>
- Yang, Y., Pan, M., Lin, P., Beck, H. E., Zeng, Z., Yamazaki, D., et al. (2021). Global reach-level 3-hourly river flood reanalysis (1980–2019). *Bulletin of the American Meteorological Society*, 102(11), E2086–E2105. <https://doi.org/10.1175/BAMS-D-20-0057.1>